THE JOURNAL OF
PHYSICAL CHEMISTRY A

Article

pubs.acs.org/JPCA

Reaction Dynamics of CN Radicals in Acetonitrile Solutions

Daisuke Koyama,[†] Philip Coulter,[†] Michael P. Grubb,[†] Gregory M. Greetham,[‡] Ian P. Clark,[‡] and Andrew J. Orr-Ewing[*,†]

[†]School of Chemistry, University of Bristol, Cantock's Close, Bristol BS8 1TS, U.K.

[‡]Central Laser Facility, Research Complex at Harwell, Science and Technology Facilities Council, Rutherford Appleton Laboratory, Harwell Oxford, Didcot, Oxfordshire OX11 0QX, U.K.

Supporting Information

ABSTRACT: The bimolecular reactions that follow 267 nm ultraviolet photolysis of ICN in acetonitrile solution have been studied using transient absorption spectroscopy on the picosecond time scale. Time-resolved electronic absorption spectroscopy (TEAS) in the ultraviolet and visible spectral regions observes rapid production and loss (with a decay time constant of 0.6 ± 0.1 ps) of the photolytically generated free CN radicals. Some of these radicals convert to a solvated form which decays with a lifetime of 8.5 ± 2.1 ps. Time-resolved vibrational absorption spectroscopy (TVAS) reveals that the free and solvated CN-radicals undergo geminate recombination with I atoms to make ICN and INC, H atom abstraction reactions, and addition reactions to solvent molecules to make $C_3H_3N_2$ radical species. These radical products have a characteristic absorption band at 2036 cm^{-1} that shifts to 2010 cm^{-1} when ICN is photolyzed in CD_3CN. The HCN yield is low, suggesting the addition pathway competes effectively with H atom abstraction from CH_3CN, but the delayed growth of the $C_3H_3N_2$ radical band is best described by reaction of solvated CN radicals through an unobserved intermediate species. Addition of methanol or tetrahydrofuran as a cosolute promotes H atom abstraction reactions that produce vibrationally hot HCN. The combination of TEAS and TVAS measurements shows that the rate-limiting process for production of ground-state HCN is vibrational cooling, the rate of which is accelerated by the presence of methanol or tetrahydrofuran.

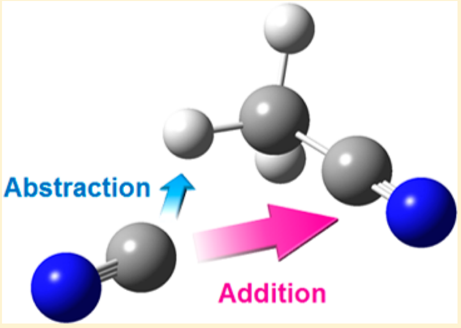

1. INTRODUCTION

Elementary bimolecular chemical reactions are the basic steps of many more-complex chemical processes; consequently, their rates, mechanisms and reaction dynamics have been extensively studied by both experimental and theoretical methods.[1,2] Many of these studies have concentrated on radical reactions in the gas phase. Under gas-phase conditions dominated by isolated collisions, competing reaction pathways can be distinguished, as can the release of excess energy from exothermic reactions into specific translational, rotational, vibrational or electronic degrees of freedom of the reaction products. These types of observation reveal detailed information about the structures of key intermediates along the reaction path.

Reactive collisions cannot be considered to occur in isolation in the liquid phase, where many important synthetic and biochemical processes take place. Instead, the surrounding solvent interacts continuously with the reacting species and can modify energy barriers, reaction pathways, product yields and the flow of any energy released.[3] These interactions occur on ultrafast (femtosecond to picosecond) time scales, but nonequilibrium reaction dynamics reminiscent of the gas-phase can persist if reactive events are fast enough to compete with the response of the surrounding solvent.[4−8]

To investigate some of the effects of solvent on the dynamics and pathways of bimolecular reactions, ultraviolet (UV) photolysis of dissolved cyanogen iodide (ICN) has been employed as a source of CN radicals.[4,5] These reactive radicals typically abstract hydrogen atoms from organic molecules as shown by eq 1, and the reactions with alkanes have been extensively studied in the gas phase.[9−14]

$$CN + RH \rightarrow HCN(v_1, v_2, v_3) + R \qquad (1)$$

Here, (v_1,v_2,v_3) denotes the number of quanta of the three vibrational modes of HCN, the C−N stretch (v_1), the bend (v_2), and the C−H stretch (v_3). These reactions typically release more than 100 kJ mol^{-1} of energy, and a significant fraction flows into the internal vibrational modes of the products. The potential energy surfaces (PESs) for these reactions have early and low energy barriers, with a flat angular dependence at the transition state.[15,16] Consequently, the energy released by the reaction excites the HCN in the C−H stretching and bending vibrations.

Reactions of the type illustrated by eq 1 have also been investigated in solution in common chlorinated organic solvents. For example, Orr-Ewing and co-workers explored the reaction dynamics of CN radicals with various organic molecules (cyclohexane, d_{12}-cyclohexane, tetramethylsilane, tetrahydrofuran (THF), acetone) in chloroform and dichloro-

Received: November 2, 2015
Revised: December 3, 2015
Published: December 4, 2015

DOI: 10.1021/acs.jpca.5b10720
J. Phys. Chem. A 2015, 119, 12924−12934

methane using time-resolved vibrational absorption spectroscopy (TVAS).[17−21] The experimental measurements demonstrated that the degree of vibrational excitation of the nascent products is reduced in the liquid phase, but signatures of the gas-phase dynamics remain. Complete quenching of nascent vibrational excitation by interaction with the solvent bath can take tens to hundreds of picoseconds in chloroform and dichloromethane solutions.[4,5,17−19,22] Modifications of the reaction mechanism by interactions with the solvent bath include formation of complexes between CN radicals and solvent molecules.[23,24]

The current study extends these prior investigations to reactions of CN radicals in acetonitrile (CH_3CN or CD_3CN), which is chosen because it is a more strongly interacting solvent than chloroform and dichloromethane. The response of acetonitrile molecules to changes in polarity in solutes is known to be fast,[25,26] with subpicosecond restructuring of the solvent shell. We consider reactions of the CN radical with both the acetonitrile solvent and with THF or methanol (CH_3OH) present as cosolutes. We observe the production and loss of CN radicals by transient electronic absorption spectroscopy (TEAS), and use TVAS to monitor the outcomes of competing chemical reactions. Abstraction reactions of the type represented by eq 1 occur, but we also report evidence of a pathway involving addition of a CN radical to the nitrile group of the acetonitrile solvent.

2. EXPERIMENTAL DETAILS

Transient absorption spectroscopy experiments were performed using the ULTRA laser system at the Central Laser Facility of the Rutherford Appleton Laboratory[27] or an ultrafast laser system at the University of Bristol. The details of each system and our experimental methods have been described previously;[19,28] therefore, only a brief description relating directly to the current study is provided here.

ICN (98%; Acros Organics) was recrystallized from toluene (Sigma-Aldrich, analytical grade) solution before use. The ICN samples were prepared as 290 mM solutions in CH_3CN, CD_3CN, THF in CH_3CN, neat THF, or methanol in CH_3CN (all solvents from Sigma-Aldrich, analytical grade; CD_3CN-d_3 99.5 atom %). Measurements were carried out in a Harrick cell with a 380-μm thick PTFE spacer and CaF_2 windows and the 5−10 mL sample solutions were circulated by a peristaltic pump. The reactions were initiated by a 267 nm UV pulse (duration ~50 fs; 1 μJ per pulse) and probed by transient infrared (IR) absorption using a ~500 cm^{-1} (~300 cm^{-1} for the Bristol laser system) bandwidth IR laser pulse for TVAS experiments or by transient UV/vis absorption using a broadband white light continuum (340−620 nm) for TEAS experiments. The chosen ICN concentration gave an absorbance of 1.0 at the 267 nm excitation wavelength.

Density functional theory (DFT) calculations of harmonic vibrational frequencies were performed using the Gaussian 09 package and the B3LYP density functional with the 6-311+ +G(3df,3pd) basis set.[29] This method was chosen because of its good balance between computational efficiency and reliability, as well as the availability of scaling factors for infrared frequency calculations. DFT calculations using the BPW91 functional were also conducted to confirm the results obtained using the B3LYP method. Various types of methods for calculation of harmonic vibrational frequencies were tested, but calculated frequencies obtained with the BPW91 functional provided the best results for our system without using a scaling factor, as ascertained by comparison with steady state FT-IR spectrum of stable compounds such as CH_3CN, CD_3CN, and HCN.

3. RESULTS AND DISCUSSION

Unravelling the chemistry that occurs following UV photolysis of ICN in acetonitrile solution requires information from both TEAS and TVAS experiments. The TEAS measurements identify the production, solvation and loss of CN radicals and are reported first because they establish the time scales for reactive removal of CN. The TVAS measurements examine the products of CN radical reactions, as well as geminate recombination of CN with I atoms. Comparison of the product-formation time scales with the CN-loss rates obtained by TEAS reveals reactive pathways and provides evidence for intermediate species that are not directly observed in our experiments. We concentrate first on the ICN/CH_3CN and ICN/CD_3CN solutions to establish the processes that occur when CN is produced photolytically in acetonitrile, and then consider the changes that result from addition of THF or methanol.

3.1. TEAS of Solution of ICN in CH_3CN Following 267 nm Excitation. Figure 1 shows TEA spectra of 290 mM ICN in CH_3CN following 267 nm UV excitation. The spectra can be decomposed into three contributing features, in accord with prior analysis by Rivera et al. and illustrated for a TEA spectrum obtained at a time delay of 0.6 ps in Figure 1b.[30] We performed this decomposition in the KOALA program.[31] Figure 1c shows exponential fits to the time-dependence of the intensities of these three spectral features, and the corresponding time constants are summarized in Table 1.

A sharp band centered at 389 nm at early time delays grows within our instrument response limit (~200 fs) and decays with a time constant of 0.6 ± 0.1 ps (Figure 1c). The location of this peak matches the B ← X electronic transition of the CN radical in the gas phase, and in agreement with Rivera et al. and Crowther et al., we assign it to nonsolvated ("free") CN radicals.[23,24,30,32] In response to the decay of the nonsolvated CN radicals, we see evolution of a broad new component peaking to the shorter wavelength side of the nonsolvated CN radicals with a time constant for growth of 0.6 ± 0.1 ps. Given this correspondence between time constants, we assign this broad feature to solvated CN radicals, although a contribution from I atoms must also be considered. Similar correspondences between decay of free CN radicals and growth of solvated CN radicals are also observed in other solvent systems.[21] Following its rapid growth, the solvated CN radical absorption decays, and as Figure 1c shows, fitting this decay to a biexponential function gives time constants of 8.5 ± 2.1 and 108 ± 26 ps. The faster decay component of the solvated CN radical is attributed predominantly to reaction with CH_3CN and, to a lesser extent, geminate recombination to ICN and INC, on the basis of TVAS results presented in section 3.2.

The third component of the spectra at short times is a broad band peaking around 580 nm and extending across much of the visible region. Similar bands were observed previously by Rivera et al. following ICN photolysis in water and ethanol and assigned to a charge-transfer (CT) band of spin−orbit excited and solvated I*($^2P_{1/2}$) atoms.[30] The corresponding band of ground-state I($^2P_{3/2}$) atoms lies to shorter wavelength and partially overlaps the solvated CN absorption band. The I* CT band decays rapidly because of spin−orbit relaxation, as shown in Figure 1c, with concomitant growth of the I($^2P_{3/2}$)-solvent CT feature expected. The evidence presented here shows that

DOI: 10.1021/acs.jpca.5b10720
J. Phys. Chem. A 2015, 119, 12924−12934

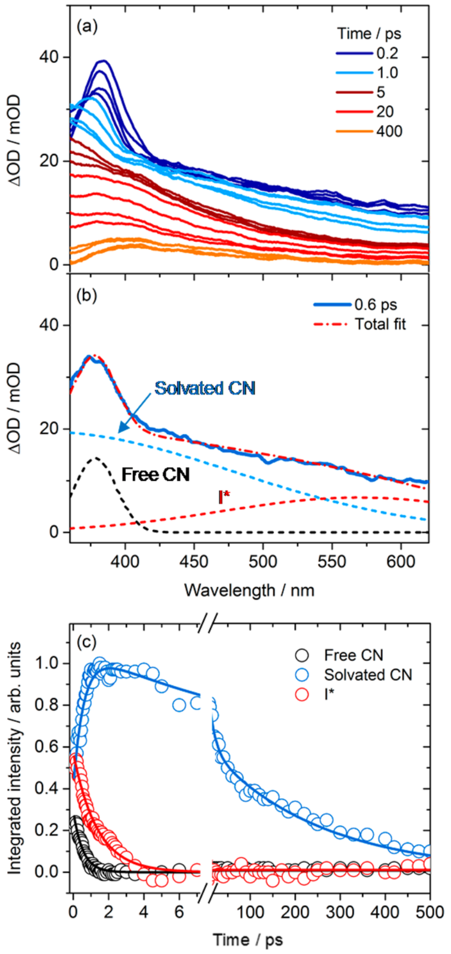

Figure 1. Transient electronic absorption spectra of 290 mM ICN in CH_3CN following 267 nm excitation and the spectral decomposition into component absorptions. (a) TEA spectra for selected time delays from 0−1300 ps, with a color code provided as an inset key. (b) Example of decomposition of the spectrum obtained at a time delay of 0.6 ps into its constituent parts. (c) Time-dependence of the free and solvated CN radical absorption bands and the I* charge-transfer band obtained from decomposition of TEA spectra. The solid lines are exponential fits with time constants reported in Table 1. The long-time decay of intensity in the region spanned by the solvated CN band is a consequence of an overlapping solvent-I atom charge transfer band.

Table 1. Time Constants Obtained from Exponential Fits to Time-Dependent Intensity Data from TEA Spectra for Bands Labelled as Free CN, Solvated CN and I*.[a]

	τ_1/ps	τ_2/ps	τ_3/ps
free CN	0.6 ± 0.1		
solvated CN	0.6 ± 0.1[b]	8.5 ± 2.1	108 ± 26[c]
$I^*(^2P_{1/2})$	1.5 ± 0.1		

[a] Uncertainties are 2 SD from the fits. [b] This time constant corresponds to growth of the spectral feature. [c] Overlapping contribution from $I(^2P_{3/2})$ atoms.

the early time temporal behavior of the broad band extending from the near-UV to the visible region is more consistent with assignment to loss of solvated CN radicals than to ground-state I atoms. However, the slower (108 ± 26 ps) decay component of this feature is not observed in experimental studies of BrCN photolysis in acetonitrile,[21] and is therefore attributed to the $I(^2P_{3/2})$ atoms. These ground-state I atoms are lost by diffusive recombination with other radical or atomic species, for example forming I_2.

At the longest time delays in our measurements, a spectral feature remains that is centered at 400 nm. A similar feature was reported in Dunning et al.'s recent study of ICN photolysis in acetone solutions, and was assigned to a stable CN-acetone complex.[20] One possible assignment of the 400 nm band is therefore to a CN-acetonitrile complex, but this appears to be only a partial explanation. In our ICN/acetonitrile solutions we see evidence for development of an I_3^- band centered at 365 nm even without any laser irradiation. Therefore, we interpret the 400 nm feature as a combination of a CN-acetonitrile complex absorption band and a bleach feature derived from I_3^-. The interference from the I_3^- bleach becomes more significant when THF is added and valuable information is lost in CH_3CN/THF solutions. Therefore, TEA spectra for solutions containing THF are not shown and discussed.

3.2. TVAS of Solutions of ICN in CH_3CN Following 267 nm Excitation.

One pathway for reaction of CN radicals with CH_3CN might involve the H atom abstraction of eq 2 in which HCN is a product. TVAS observations of these HCN products were restricted to the C−N stretching region at wavenumbers around 2050 cm^{-1} because of strong interferences in the C−H stretching region from CH_3CN modes.

$$CN + CH_3CN \rightarrow HCN + CH_2CN \qquad (2)$$

Examples of TVA spectra obtained by photolysis of 290 mM ICN in CH_3CN and CD_3CN are shown in Figure 2, panels a and b. None of the time-dependent spectral features are seen in experiments conducted on CH_3CN or CD_3CN samples without ICN solute. A bleach of the ICN absorption band induced by the pump laser is not shown in the figure, but it is observed as a negative-going signal at 2167 cm^{-1} in both solvents and shows almost no recovery. The band at 2118 cm^{-1} in the CD_3CN solution is attributed to the solvent by comparison with steady state FT-IR spectra. This negative-going band increases in depth with greater delay times, which suggests reactive loss of solvent molecules because the transient feature is not observed in the absence of ICN. The time-dependence of the integrated band intensity is shown in Figure 2(c). Following a rapid onset of the bleach of the CD_3CN band, its further development is fitted well by a biexponential function with time constants of 8.7 ± 1.8 ps and 82 ± 30 ps.

The subpicosecond initial growth of the CD_3CN bleach suggests some reactive removal by the free CN radicals produced by ICN photolysis. The subsequent 8.7 ps time constant for the development of the CD_3CN bleach feature matches that obtained from TEAS data for decay of solvated CN radicals in CH_3CN (Table 1). This correspondence supports the reaction of acetonitrile with solvated CN radicals as a contributing cause of the time-dependence of both the TEAS and TVAS bands. The cause of the longer-time loss of CD_3CN (with τ_2 = 82 ± 30 ps) is uncertain, but the relative amplitudes of the different components of the time-evolution of this band show that this is a minor pathway compared to the reactive removal by CN radicals.

The band centered at 2068 cm^{-1} is assigned to the C≡N stretching band of INC(ν = 0) formed by geminate recombination on the basis of our and others' prior observations.[17−21,33−36] This assignment is further supported by the fact there is no isotope shift when CH_3CN is replaced by CD_3CN. The INC(ν = 0) band grows with a time constant of 7.7 ± 0.7 ps in CH_3CN that is commensurate with the loss of

DOI: 10.1021/acs.jpca.5b10720
J. Phys. Chem. A 2015, 119, 12924−12934

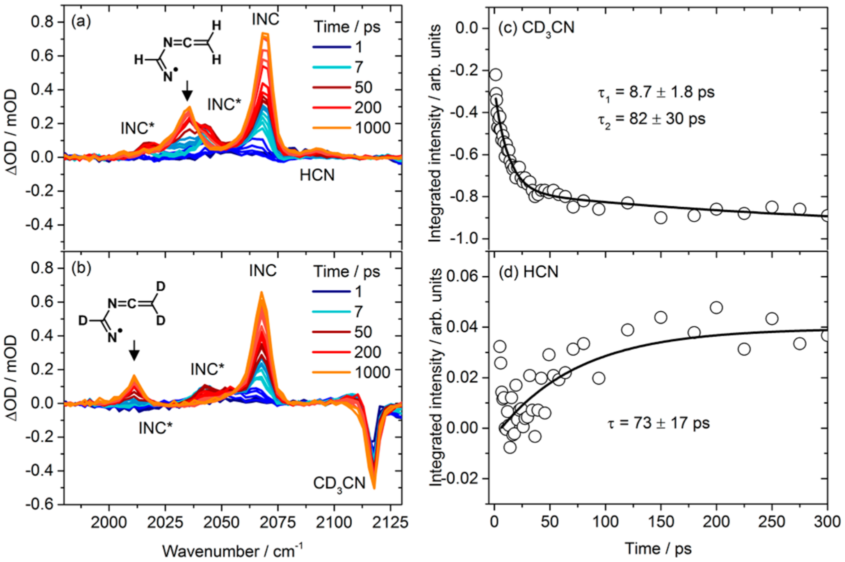

Figure 2. Transient vibrational absorption spectra obtained following 267 nm UV excitation of 290 mM ICN in (a) CH_3CN and (b) CD_3CN obtained in the 1980–2130 cm^{-1} range. Inset color keys identify spectra obtained at selected time delays. Band assignments are indicated and discussed further in the main text. Time-dependences of integrated band intensities are shown for (c) the CD_3CN band at 2118 cm^{-1} and (d) the weak HCN band in CH_3CN at 2092 cm^{-1}. Exponential or biexponential fits to these time-dependent intensities give the reported time constants.

Table 2. Observed and Calculated Fundamental Infrared Frequencies and Intensities of the $H_2C{=}C{=}NCHN$ and $D_2C{=}C{=}NCDN$ Radicals formed by CN Addition to Acetonitrile

	observed in TVAS	B3LYP/6-311++G(3df,3pd)		BPW91/6-311++G(3df,3pd)	
	frequency/cm^{-1}	frequency/cm^{-1} [a]	intensity/km mol^{-1}	frequency/cm^{-1}	intensity/km mol^{-1}
$H_2C{=}C{=}NCHN$	2036	2016	567	2043	408
$D_2C{=}C{=}NCDN$	2010	1992	481	2021	345

[a] Frequencies calculated at the B3LYP level were multiplied by a factor of 0.9604.[39]

CN seen by TEAS with $\tau = 8.5 \pm 2.1$ ps, followed by a more gradual increase with a time constant of 341 ± 21 ps. In addition to the fundamental C−N stretching band of INC, we assign the peaks at 2043 and 2018 cm^{-1} to absorption from the $\nu = 1$ and 2 vibrational levels of the C≡N stretching mode of INC.[21] These bands are shifted to lower wavenumber than the fundamental band by intervals corresponding to the 12.5 cm^{-1} diagonal anharmonicity of this mode deduced from electronic structure calculations.[21] The value is also consistent with the anharmonicity of the CN radical vibration.[37] These two hot bands grow with the same time constants as the fundamental INC band, and decay with time constants of 282 ± 67 ps for the INC($\nu = 2$) band and 630 ± 76 ps for the INC($\nu = 1$) band that are in a ratio consistent with expectations from Landau−Teller theory.[38] The geminate recombination is therefore concluded to produce some vibrationally excited INC molecules, and competes with ICN, but is a minor recombination channel (accounting for only a few percent of the dissociated I atoms and CN radicals) observable only because of the large IR transition dipole moment of the C≡N stretching mode.[33] We estimate that approximately 30% of the initially formed INC is vibrationally excited in the C≡N stretching mode by comparing IR band intensities at early time delay (∼15 ps), with account taken for differences in the transition dipole moments for the bands.

The bands at 2036 cm^{-1} in CH_3CN and 2010 cm^{-1} in CD_3CN grow with time constants of 50 ± 3 ps and 50 ± 2 ps respectively if their time-dependent intensities are fitted to single exponential functions. The agreement between time constants indicates that these peaks derive from corresponding reactions in CH_3CN and CD_3CN. The isotope shift of 26 cm^{-1} demonstrates that the responsible species contains H or D atoms and this species is derived from CH_3CN or CD_3CN because these peaks are not observed in other solvents such as chloroform or dichloromethane.[17−21] Assignment to CH_2CN (or CD_2CN) products of reaction 2 was discounted because we conducted experiments on the UV photolysis of ICH_2CN in acetonitrile and did not observe the same spectral features. DFT calculations also fail to predict CH_2CN/CD_2CN bands in proximity to the observed features and with the correct isotope shifts. These measurements and calculations are reported in the Supporting Information. Consequently, we assign these peaks to the radical products of addition of CN to acetonitrile:

$$CN + CH_3CN(CD_3CN) \rightarrow C_3H_3N_2^{\bullet}(C_3D_3N_2^{\bullet}) \qquad (3)$$

Our DFT calculations identified numerous $C_3H_3N_2^{\bullet}$ (or $C_3D_3N_2^{\bullet}$) adducts lower in energy than separated CN and CH_3CN (see Supporting Information for further details), but on the basis of computed vibrational frequencies, isotope shifts and band intensities, our preferred assignment is to $H_2C{=}C{=}NCHN$ in CH_3CN and $D_2C{=}C{=}NCDN$ in CD_3CN, with the structures shown in Figure 2, parts a and b. The computed wavenumbers and intensities of the bands of these two structures in this spectral region are reported in Table 2; the large transition dipole moments facilitate observation of these bands in our TVA spectra. The observed vibrational mode corresponds to stretching of the central C═N bond. Addition of CN to the C atom of the nitrile group in acetonitrile is also

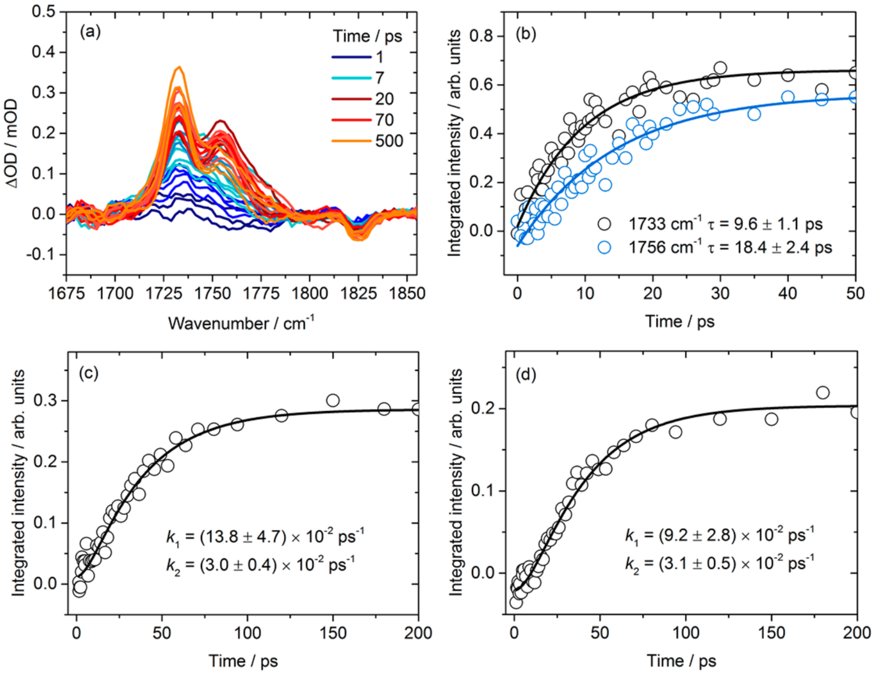

Figure 3. (a) Transient vibrational absorption spectra of UV-photoexcited 290 mM ICN in CH_3CN in the 1675−1850 cm^{-1} range. A small bleach feature observed at around 1825 cm^{-1} is attributed to a CH_3CN solvent band. (b) Time dependence of the bands at 1733 and 1756 cm^{-1}. The lower two panels show integrated band intensities and fits to the sequential reaction model of eq 4 for (c) the $H_2C{=}C{=}NCHN$ band at 2036 cm^{-1} in CH_3CN and (d) the $D_2C{=}C{=}NCDN$ band at 2010 cm^{-1} in CD_3CN both of which are evident in Figure 2.

plausible, but the computed vibrational transition dipole moments of the resulting $CH_3C(N^\bullet)CN$ radicals are 1 or 2 orders of magnitude smaller in our spectroscopic window (see Supporting Information). These possible alternative reaction products may therefore be overlooked.

The time constants for formation of the radical adduct products (~50 ps) are significantly slower than the expected reaction time scale of ~8.5 ps for solvated CN (Table 1). TVAS data obtained in other wavenumber regions indicate that there are some product bands that grow with faster time constants in the 9−20 ps range. Two such examples are bands centered at 1733 and 1756 cm^{-1}, as shown in Figure 3 for ICN photolysis in CH_3CN. The slower buildup of intensity on the bands at 2036 cm^{-1} (in CH_3CN) and 2010 cm^{-1} (in CD_3CN) can be understood if the proposed $H_2C{=}C{=}NCHN$ or $D_2C{=}C{=}NCDN$ products are not directly produced by addition of CN to the acetonitrile molecule, but are instead the result of isomerization or quenching of an initially formed intermediate. The postulated intermediate is not necessarily the same species as is responsible for the 1733 or 1756 cm^{-1} features. The sequential kinetic model of eq 4 (shown for the CH_3CN case, and with CN denoting a solvated form of the radical) provides a good account of the observed band intensities, with fitted rate coefficients of $k_1 = (13.8 \pm 4.7) \times 10^{-2}$ ps^{-1} and $k_2 = (3.0 \pm 0.4) \times 10^{-2}$ ps^{-1} for CH_3CN and $k_1 = (9.2 \pm 2.8) \times 10^{-2}$ ps^{-1} and $k_2 = (3.1 \pm 0.5) \times 10^{-2}$ ps^{-1} for CD_3CN solutions.

$$\begin{aligned} &\mathrm{CN} + \mathrm{CH_3CN} \xrightarrow{k_1} \mathrm{CN{-}CH_3CN\ adduct} \\ &\xrightarrow{k_2} \mathrm{H_2C{=}C{=}NCHN} \end{aligned} \tag{4}$$

Fits to this model are shown in Figure 3, parts c and d. The k_1 values agree within the 2 SD uncertainties with the rate coefficient obtained from growth of the band at 1733 cm^{-1} seen in the TVA spectra in Figure 3a ($k_1 = 1/\tau_1 = (10.4 \pm 1.2) \times 10^{-2}$ ps^{-1}), as well as the 8.5 ± 2.1 ps decay of solvated CN radicals and the 8.7 ± 1.8 ps growth of the CD_3CN bleach. A common time scale is thus observed for CN radical consumption by these competing reaction and recombination pathways. The isomerization or quenching step to $H_2C{=}C{=}NCHN$ or $D_2C{=}C{=}NCDN$ radicals is estimated to occur with a $\tau_2 = 1/k_2 \approx 33$ ps time constant. The band at 1756 cm^{-1} (Figure 3, parts a and b) grows with a time constant of 18.4 ± 2.4 ps when fitted by a single exponential function and its growth is slower than the expected reaction time scale. The carrier of this band might therefore be formed through other sequential process associated with the addition reaction 3.

The weak TVAS band at 2092 cm^{-1} in CH_3CN (Figure 2a) is assigned to the fundamental C≡N stretching band of the ground vibrational state of HCN (denoted by HCN(0)) formed by reaction 2. This assignment is made on the basis that the peak position agrees with a steady state FT-IR spectrum of HCN obtained by photolysis of ICN in CH_3CN, and is not observed for experiments conducted in CD_3CN. The time-dependent integrated band intensities plotted in Figure 2d suggest positive but declining intensities at the earliest time delays (the first 5 ps) followed by a growth with a time constant of 73 ± 17 ps when fitted by a single exponential function. The resulting integrated absorbance remains constant from approximately 150 ps until the limit of our experimental time delay (3 ns). The early time positive intensity may be a consequence of baseline noise affecting the low HCN band intensity, or could be a signature of vibrationally hot products formed on this time scale.

The intensity of the HCN fundamental band at late times for measurements conducted in CH_3CN is significantly weaker than we observed for experiments conducted in other organic solvents including $CHCl_3$, CH_2Cl_2 and THF (see section 3.4).[17−19] We attribute the apparently low yield of HCN from the abstraction reaction 2 to the competitive addition reaction

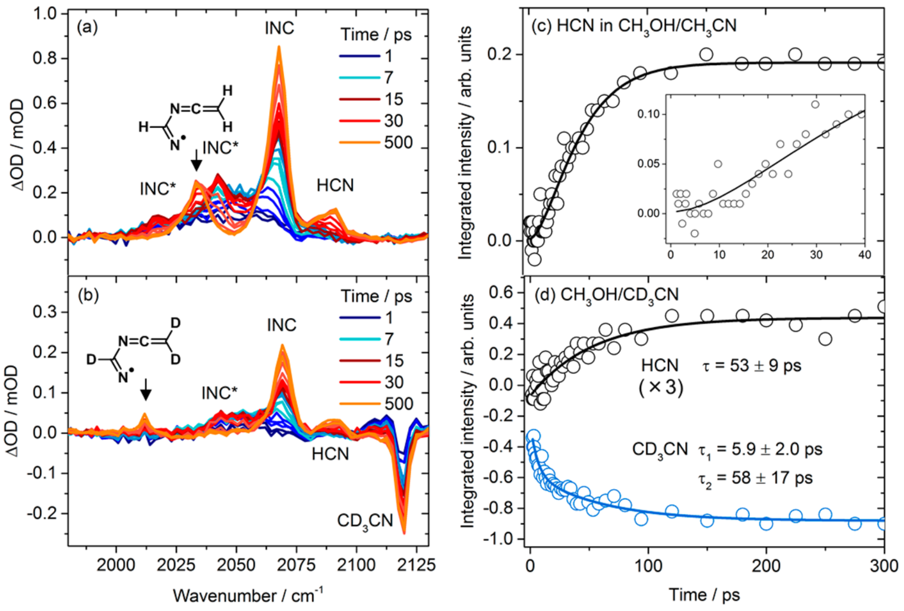

Figure 4. (a) Transient vibrational absorption spectra of 290 mM ICN in 2.0 M CH_3OH/CH_3CN solutions. The feature at 2090 cm^{-1} is assigned to HCN(0). The features at 2068, 2043, and 2018 cm^{-1} are assigned to the fundamental band and vibrational hot bands of INC.[21] The band at 2035 cm^{-1} is assigned to $H_2C{=}C{=}NCHN$. (b) Transient vibrational absorption spectra of 290 mM ICN in 2.0 M CH_3OH/CD_3CN solutions. The features at 2010 and 2118 cm^{-1} are assigned to $D_2C{=}C{=}NCDN$ and CD_3CN respectively. (c) Time dependence of the HCN(0) band at 2090 cm^{-1} in a 2.0 M CH_3OH/CH_3CN solution. The solid line is a fit to a sequential kinetic model described in the text. The inset shows an expanded view of the first 40 ps. (d) Time dependence of the HCN(0) band at 2090 cm^{-1} (black) and the CD_3CN band at 2118 cm^{-1} (blue) in a 2.0 M CH_3OH/CD_3CN solution. The intensities for the HCN(0) band are multiplied by 3 for clarity. The solid lines are fits to a single exponential function for the HCN(0) band and to a biexponential function for the CD_3CN band.

shown in eqs 3 and 4. The time constant for growth of the HCN fundamental band intensity of 73 ± 17 ps is much larger than the ~8.5 ps time constant for the loss of solvated CN radicals observed in TEAS and CD_3CN in TVAS, indicating that the bimolecular reaction is not the rate limiting process in HCN(0) formation. Instead, we attribute the slower rate of buildup of HCN(0) to relaxation of HCN molecules formed in vibrationally excited levels by the exothermic H atom abstraction reaction. Further justification for this interpretation is presented in the following sections.

3.3. Effect of Adding Methanol on HCN Formation in Acetonitrile.

The data presented in section 3.2 showed that the peak intensity of the HCN fundamental band in CH_3CN solution is weak because of competition between H atom abstraction and addition reaction pathways. We explored this competition further by adding organic cosolutes to the ICN solutions in acetonitrile, the first of which was chosen to be methanol.

Measurements of TVA spectra of ICN in CH_3OH/CH_3CN solutions were restricted to relatively low CH_3OH concentrations (≤2.0 M) because unidentified deposits developed on the CaF_2 windows of the Harrick cell during laser irradiation of samples with higher CH_3OH concentrations. Figure 4 illustrates TVA spectra of 290 mM ICN in a 2.0 M solution of CH_3OH in CH_3CN (a) and CH_3OH in CD_3CN (b) with indications of peak assignments. The shapes and the peak positions for components of the spectra are all similar to those observed for ICN photolysis in neat CH_3CN or CD_3CN. The most obvious change is the increase of the HCN(0) band intensity at 2090 cm^{-1}, for which the kinetics in CH_3OH/CH_3CN solution are shown in Figure 4c following spectral decomposition in KOALA,[31] suggesting H atom abstraction from CH_3OH is faster than that from CH_3CN and can compete with the addition reaction 4.

The HCN band rises with a time constant of 39 ± 3 ps following an initial induction of ~10 ps and shows an almost constant absorbance after ~120 ps. This kinetic behavior, with a delayed onset to the growth of the band, indicates that higher vibrational levels of the HCN are formed from the reaction and that vibrational relaxation processes from the higher levels to the ground state take place on this time scale, as previously was argued by Rose et al.[17,18] The HCN(0) band intensities are well fitted by a stepwise kinetic model describing this behavior (Figure 4c). Figure 4d shows the kinetics of the HCN(0) and CD_3CN solvent bands in a 2.0 M CH_3OH/CD_3CN solution. As is the case for neat CD_3CN, the CD_3CN band shows a negative-going feature with a time-dependence that is well fitted by a biexponential function, but with time constants of 5.9 ± 2.0 and 58 ± 17 ps. The faster time constant agrees with that for formation of INC (τ = 6.4 ± 0.9 ps), which is to be expected for two competing processes involving consumption of solvated-CN radicals. The poorer signal-to-noise ratios on HCN band intensities for measurements in the CH_3OH/CD_3CN solution prevent analysis using the stepwise kinetic model applied to HCN production in the CH_3OH/CH_3CN solution.

The key time constants deduced from analysis of UV-excited ICN/acetonitrile and ICN/2.0 M CH_3OH/acetonitrile solutions are reported in Table 3. These time constants can be inverted to give pseudo-first order rate coefficients because both acetonitrile and CH_3OH are in considerable excess over CN radicals.

Figure 5 shows the reaction rate coefficients deduced in this way by fitting HCN(0) rise times to single-exponential functions for solutions of different CH_3OH concentration in

Table 3. Summary of the Time Constants for Solvated CN Radicals, CD_3CN and HCN(0) in Acetonitrile and 2.0 M CH_3OH/Acetonitrile Solutions

	τ_1/ps	τ_2/ps
decay of solvated CN radicals in neat CH_3CN	8.5 ± 2.1	108 ± 26[a]
formation of HCN(0) in neat CH_3CN	73 ± 17	
formation of HCN(0) in 2.0 M CH_3OH/CH_3CN	39 ± 3	
decay of CD_3CN in neat CD_3CN	8.7 ± 1.8	82 ± 30
decay of CD_3CN in 2.0 M CH_3OH/CD_3CN	5.9 ± 2.0	58 ± 17
formation of HCN(0) in 2.0 M CH_3OH/CD_3CN	53 ± 9	

[a] Attributed to an overlapping solvent-I atom CT band.

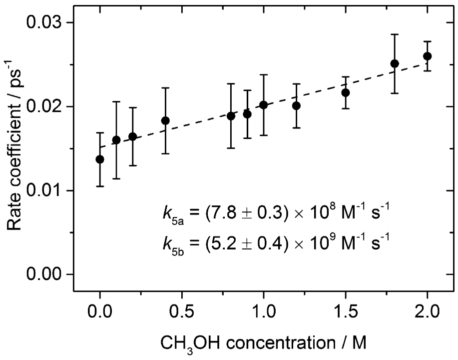

Figure 5. Pseudo first order rate coefficients for HCN(0) formation as a function of CH_3OH concentration. The rate coefficients are obtained as reciprocals of exponential time constants for the HCN(0) growth.

CH_3CN. The first-order rate coefficients depend linearly on CH_3OH concentration. The HCN band intensities also increase as the concentration of CH_3OH rises, indicating successful competition of the CN + CH_3OH reaction with the addition of CN radicals to acetonitrile molecules. The time constant for removal of CD_3CN in 2.0 M CH_3OH/CD_3CN solutions is a measure of the rate at which CN radicals are consumed by all competing pathways including H atom abstraction from CH_3OH. This time constant is significantly smaller than that for HCN(0) growth under the same conditions. The abstraction reaction is therefore not the rate-determining step; instead, production of HCN(0) is controlled by the vibrational relaxation of nascent, internally hot HCN* molecules. The pseudo first order rate coefficients therefore describe how addition of CH_3OH accelerates this vibrational relaxation. The bimolecular reactions can be with either CH_3CN or CH_3OH molecules in the solution to produce HCN* which is then quenched by two mechanisms:

$$HCN^* + CH_3CN \xrightarrow{k_{5a}} HCN(0) + CH_3CN \tag{5a}$$

$$HCN^* + CH_3OH \xrightarrow{k_{5b}} HCN(0) + CH_3OH \tag{5b}$$

If these relaxation steps are indeed rate limiting, the rate of HCN(0) formation is given by

$$\frac{d[HCN(0)]}{dt} = k_5'[HCN^*] \tag{6}$$

With the pseudo first order rate coefficient:

$$k_5' = k_{5a}[CH_3CN] + k_{5b}[CH_3OH] \tag{7}$$

A linear fit to a plot of k_5' against $[CH_3OH]$ is shown in Figure 5 and gives a gradient of $(5.2 \pm 0.4) \times 10^{-3}$ M^{-1} ps^{-1} and an intercept of $(1.5 \pm 0.05) \times 10^{-2}$ ps^{-1}. The pseudo first order analysis therefore indicates bimolecular rate coefficients k_{5a} = $(7.8 \pm 0.3) \times 10^8$ M^{-1} s^{-1} for quenching by acetonitrile (using a molarity of neat CH_3CN of 19.1 M) and k_{5b} = $(5.2 \pm 0.4) \times 10^9$ M^{-1} s^{-1} for the quenching by CH_3OH. The signal-to-noise levels in TVAS spectra prevented a more complete interpretation of the vibrational cooling of the HCN*. However, for studies in which THF was added to the ICN/acetonitrile solutions, a more detailed analysis was possible, as is discussed in section 3.4.

3.4. Effect of Adding Tetrahydrofuran on HCN Formation in Acetonitrile.

TVAS data were obtained for ICN in CH_3CN/THF mixtures with THF concentrations in the range 0−12.3 M, the upper limit corresponding to neat THF. Figure 6 illustrates TVA spectra obtained for a solution of 290 mM ICN in neat THF, integrated band intensities, and kinetic fits. The spectra resemble those reported previously by Rose et al.[18] and the two prominent bands at 2079 and 2059 cm^{-1} are assigned to the fundamental C≡N stretching $\nu_1 = 1 \leftarrow \nu_1 = 0$ absorption of HCN, and the fundamental C≡N stretching band of INC which is probably overlapped by underlying bands of nascent vibrationally hot HCN.[21] However, another unidentified band can also be seen at 2045 cm^{-1}. Although we always used fresh ICN and THF samples, this band was not consistently observed in every data set. Since our main interest in this study is in the effect of solvent on the dynamics of CN radicals and HCN, we do not consider this additional band further.

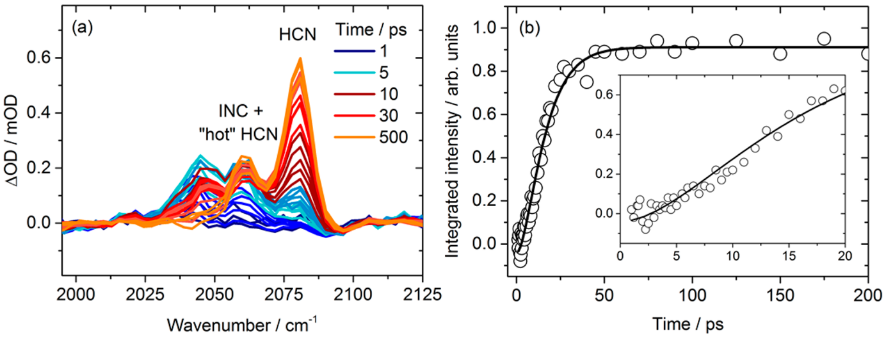

Figure 6. (a) Transient vibrational absorption spectra of a 290 mM solution of ICN in neat THF, obtained in the 1990−2125 cm^{-1} range. (b) Time dependence of the integrated intensities of the HCN fundamental C≡N stretching band at 2079 cm^{-1}. The solid line is a fit to the sequential kinetic model of eqs 8−10). The inset shows an expanded view of the first 20 ps.

The HCN band is considerably stronger relative to the INC band than we observe for reactions in acetonitrile. It rises with a time constant of 15.4 ± 0.7 ps following an initial induction of ~5 ps (Figure 6b inset) and shows an almost constant absorbance after ~50 ps, suggesting HCN is also formed via vibrationally excited HCN*.

A sequential kinetic model with vibrationally excited HCN as an intermediate species was employed in our initial analysis of the time dependence of the HCN fundamental band intensity for THF/CH_3CN solutions of various concentrations. In all cases, the time constants for growth of the HCN(0) absorption band were significantly larger than those for the loss of solvated CN radicals in an ICN/CH_3CN solution determined using TEAS. As was the case for the ICN/methanol/CH_3CN experiments reported in section 3.3, we concluded that the rate-determining step for HCN(0) growth is vibrational cooling. Moreover, we found it necessary to adopt a two-stage vibrational relaxation model to account successfully for our observations. The analysis model we adopt is therefore summarized by eqs 8−10, which incorporate reactive production of highly vibrationally excited HCN** products which undergo stepwise relaxation to HCN* and finally to ground state HCN products by interaction with either CH_3CN or THF molecules in the solution.

$$\mathrm{CN} + \mathrm{CH_3CN}/c\text{-}\mathrm{C_4H_8O} \overset{k_8}{\rightarrow} \mathrm{HCN^{**}} + \mathrm{CH_2CN}/c\text{-}\mathrm{C_4H_7O} \quad (8)$$

$$\mathrm{HCN^{**}} + \mathrm{CH_3CN} \overset{k_{9a}}{\rightarrow} \mathrm{HCN^{*}} + \mathrm{CH_3CN} \quad (9a)$$

$$\mathrm{HCN^{**}} + c\text{-}\mathrm{C_4H_8O} \overset{k_{9b}}{\rightarrow} \mathrm{HCN^{*}} + c\text{-}\mathrm{C_4H_8O} \quad (9b)$$

$$\mathrm{HCN^{*}} + \mathrm{CH_3CN} \xrightarrow{k_{10a}} \mathrm{HCN(0)} + \mathrm{CH_3CN} \quad (10a)$$

$$\mathrm{HCN^{*}} + c\text{-}\mathrm{C_4H_8O} \xrightarrow{k_{10b}} \mathrm{HCN(0)} + c\text{-}\mathrm{C_4H_8O} \quad (10b)$$

On the basis of the above kinetic model, the HCN* and HCN(0) formation rates are given by

$$\frac{\mathrm{d[HCN^*]}}{\mathrm{d}t} = \{k_{9a}[\mathrm{CH_3CN}] + k_{9b}[\mathrm{THF}]\}[\mathrm{HCN^{**}}] \quad (11)$$

$$\frac{\mathrm{d[HCN(0)]}}{\mathrm{d}t} = \{k_{10a}[\mathrm{CH_3CN}] + k_{10b}[\mathrm{THF}]\}[\mathrm{HCN^{*}}] \quad (12)$$

We observe the buildup of ground-state HCN(0) by TVAS, regardless of whether it forms from CN radical reactions with CH_3CN or THF, so these reactions are not distinguished in 8 but the experimental data demonstrate that the reaction with THF dominates. The reactive step is significantly faster than the vibrational relaxation processes, and a reduced model that describes our observations is therefore

$$\mathrm{CN} \xrightarrow{fast} \mathrm{HCN^{**}} \overset{k'_9}{\rightarrow} \mathrm{HCN^{*}} \overset{k'_{10}}{\rightarrow} \mathrm{HCN(0)} \quad (13)$$

in which k'_9 and k'_{10} are pseudo-first order rate coefficients for vibrational relaxation. These two first-order rate coefficients relate to the bimolecular rate coefficients for reactions 9 and 10 via:

$$k'_9 = k_{9\mathrm{a}}[\mathrm{CH_3}CN] + k_{9\mathrm{b}}[\mathrm{THF}] \quad (14)$$

$$k'_{10} = k_{10\mathrm{a}}[\mathrm{CH_3CN}] + k_{10\mathrm{b}}[\mathrm{THF}] \quad (15)$$

Fits of the rise of the HCN(0) band intensity to the model of eq 13 return two rate coefficient values but do not distinguish k'_9 and k'_{10}. We therefore assign the larger of the two rate coefficient values to the first vibrational relaxation step (9), on the basis that the Landau−Teller model predicts vibrational quenching rates in solution that increase with the vibrational quantum number. The fits were performed using TVAS data obtained at several THF concentrations in acetonitrile. Figure 7 shows the derived pseudo first-order rate coefficients (k'_9 and k'_{10}). Both rate coefficients depend linearly on THF concentration. The gradients of the best fit lines in Figure 7 are $(8.5 \pm 0.6) \times 10^{-3}$ M^{-1} ps^{-1} and $(7.2 \pm 0.3) \times 10^{-3}$ M^{-1} ps^{-1} for vibrational relaxation steps 9b and 10b, respectively. The corresponding intercepts are $(3.7 \pm 0.2) \times 10^{-2}$ ps^{-1} and $(1.2 \pm 0.1) \times 10^{-2}$ ps^{-1}. From these values and the concentration of neat CH_3CN, the bimolecular relaxation rate coefficients are deduced to be $k_{9\mathrm{a}} = (1.9 \pm 0.1) \times 10^9$ M^{-1} s^{-1}, $k_{9\mathrm{b}} = (8.5 \pm 0.6) \times 10^9$ M^{-1} s^{-1}, $k_{10\mathrm{a}} = (6.2 \pm 0.3) \times 10^8$ M^{-1} s^{-1} and $k_{10\mathrm{b}} = (7.2 \pm 0.3) \times 10^9$ M^{-1} s^{-1}. The exact nature of HCN** is uncertain, but it corresponds to HCN vibrationally excited either with two (or more) quanta of the same mode, or with quanta in each of two or more modes.

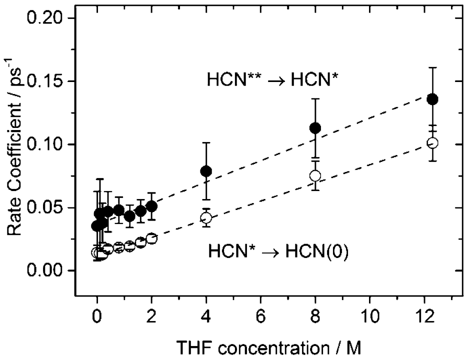

Figure 7. Pseudo-first order rate coefficients for HCN* (filled circles) and HCN(0) (open circles) formation as a function of THF concentration in acetonitrile solutions. The rate coefficients are obtained by fitting the HCN(0) kinetics to a sequential model described in the text.

We also fitted the HCN kinetics in the THF/CH_3CN solution systems with a single exponential function to compare directly with the bimolecular rate coefficient obtained in the CH_3OH/CH_3CN solution systems. Bimolecular rate coefficients for HCN(0) production of $k_{10a} = (6.7 \pm 0.4) \times 10^8$ M^{-1} s^{-1} and $k_{10b} = (4.5 \pm 0.3) \times 10^9$ M^{-1} s^{-1} are deduced. The vibrational relaxation rate coefficients for each solvent are summarized in Table 4.

The bimolecular rate coefficient values for quenching to HCN(0) by CH_3CN deduced from the THF/CH_3CN and the MeOH/CH_3CN measurements are in reasonable agreement and we prefer the value of $k_{10\mathrm{a}} = (6.2 \pm 0.3) \times 10^8$ M^{-1} s^{-1} obtained from the sequential kinetic model as a representative rate coefficient. The deduced rate coefficients for quenching of internally excited HCN by THF and CH_3OH are also similar, and almost an order of magnitude larger than the rate coefficient for quenching by CH_3CN. These differences arise from the couplings of the vibrational modes of HCN to the solvent modes, and hence depend on the structures and vibrational frequencies of the solvent molecules: THF and

Table 4. Summary of Bimolecular Relaxation Rate Coefficients for Vibrationally Excited HCN with CH_3CN, and with CH_3OH and THF in Acetonitrile Solutions

	HCN** → HCN* relaxation rate coefficient/M^{-1} s^{-1}	HCN* → HCN(0) relaxation rate coefficient/M^{-1} s^{-1}
CH_3CN		$(7.3 \pm 0.7) \times 10^8$ [a]
	$(1.9 \pm 0.1) \times 10^9$ [b]	$(6.2 \pm 0.3) \times 10^8$ [b]
CH_3OH		$(5.2 \pm 0.4) \times 10^9$ [c]
THF		$(4.5 \pm 0.3) \times 10^9$ [c]
	$(8.5 \pm 0.6) \times 10^9$ [b]	$(7.2 \pm 0.3) \times 10^9$ [b]

[a] From fitting with a single exponential function and averaging values for the CH_3OH/CH_3CN and THF/CH_3CN solutions, with an uncertainty that encompasses both values. [b] Fitting to the sequential kinetic model. [c] Fitting with a single exponential function.

CH_3OH solutes appear to offer acceptor modes for the HCN internal energy that are closer to resonant than those of acetonitrile. Much faster quenching by THF than by CH_3CN means that the differences in the rates of the HCN**→HCN* and HCN*→HCN(0) steps are not as pronounced.

4. CONCLUSIONS

The reactions that occur in photoexcited solutions of ICN in CH_3CN have been investigated by time-resolved absorption spectroscopy. Following irradiation at 267 nm, nonsolvated CN radicals form within the instrument response and become solvated in 0.6 ± 0.1 ps. The short time constant of the solvation compared to other solvents studied previously indicates rapid reorientation dynamics of the acetonitrile molecules surrounding the I + CN photofragments, perhaps driven by strong interactions between the CN radical and the C≡N functional group in CH_3CN. The solvated CN radicals decay with a time constant of 8.5 ± 2.1 ps, which is mostly determined by competing chemical processes that we have characterized by transient electronic and vibrational absorption spectroscopy to include geminate recombination (to ICN and INC) and reaction with solvent molecules. The contribution of reactions with the solvent is further supported by the observed loss of CD_3CN when experiments are conducted in deuterated acetonitrile. Most of the reactions appear to take place with the solvated CN radicals, although we do observe evidence for some reaction of CN radicals before they have equilibrated into solvated forms.

The yield of HCN from the reactions of CN radicals with the solvent is low in comparison to studies in other common solvents,[17−19] because a second pathway involving CN addition to the nitrile group of acetonitrile competes effectively. This addition can lead to numerous thermodynamically favored product radicals, but the evidence from our time-resolved spectra indicates production of $H_2C{=}C{=}NCHN$ following formation of an initial, unidentified radical adduct. Other radical products may form, but not be observed because they lack strong IR bands in the spectral region covered.

When THF or methanol is added to the ICN/CH_3CN solutions and the ternary mixture is photoexcited, the faster abstraction of an H atom from these cosolutes competes with the addition reaction of CN to acetonitrile. The TVAS measurements provide evidence of formation of vibrationally hot HCN, as was previously reported for CN reactions with other organic molecules in chlorinated solvents.[17−19] Our data for CN radical reactions with THF in acetonitrile are best explained by a mechanism in which the HCN forms with two or more quanta of vibrational excitation and undergoes stepwise vibrational relaxation. This relaxation is significantly accelerated by the presence of the THF.

The use of acetonitrile in place of other common solvents such as chloroform or dichloromethane opens up new pathways for CN radical reactions in solution. The competition between abstraction and addition pathways is reminiscent of the dynamics of CN radical reactions with alkenes in the gas phase,[40−43] but with the difference that the radical adduct can be stabilized by the surrounding solvent bath. Photoinduced radical chemistry in solution is known to lead to complicated reaction processes, and as the current study illustrates, some of these processes are highly dependent on the choice of solvent. Moreover, the rates of growth of absorption bands of reaction products can be controlled by either the reactive step or the cooling of nascent, internally excited product molecules. Nevertheless, the rate coefficients of several of the early time steps in these competing or sequential pathways can be unraveled by a combination of time-resolved vibrational and electronic absorption spectroscopies.

■ ASSOCIATED CONTENT

Ⓢ Supporting Information

The Supporting Information is available free of charge on the ACS Publications website at DOI: 10.1021/acs.jpca.5b10720. All experimental data are archived in the University of Bristol's Research Data Storage Facility (DOI: 10.5523/bris.1bvvhkmn0dhd61ol5zmtgyv2dk).

> TVA spectra of UV-excited ICH_2CN in CH_3CN, and computed energies, vibrational frequencies and IR band intensities of possible products of the addition of CN to CH_3CN and CD_3CN (PDF)

■ AUTHOR INFORMATION

Corresponding Author

*(A.J.O.-E.) Telephone: +44 (0)117 9287672. E-mail: A.Orr-Ewing@bristol.ac.uk.

Notes

The authors declare no competing financial interest.

■ ACKNOWLEDGMENTS

The Bristol group thanks the European Research Council (ERC, Advanced Grant 290966 CAPRI) for financial support. M.P.G. acknowledges award of a Marie Curie International Incoming Fellowship (PIIF-GA-2012-326988). The ULTRA Laser Facility is supported by the Science and Technology Facilities Council (STFC, Facility Grant ST/501784). We thank Igor V. Sazanovich and Mike Towrie (STFC Rutherford Appleton Laboratory) for assistance with the experimental measurements.

■ REFERENCES

(1) Levine, R. D. *Molecular Reaction Dynamics*. Cambridge University Press: Cambridge, U.K., 2005.

(2) *Tutorials in Molecular Reaction Dynamics*; Brouard, M., Vallance, C., Eds.; Royal Society of Chemistry: Cambridge, U.K., 2010.

(3) Elles, C. G.; Crim, F. F. Connecting Chemical Dynamics in Gases and Liquids. *Annu. Rev. Phys. Chem.* **2006**, *57*, 273−302.

(4) Orr-Ewing, A. J. Dynamics of Bimolecular Reactions in Solution. *Annu. Rev. Phys. Chem.* **2015**, *66*, 119−141.

(5) Orr-Ewing, A. J. Bimolecular Chemical Reaction Dynamics in Solution. *J. Chem. Phys.* **2014**, *140*, 090901.

(6) Glowacki, D. R.; Orr-Ewing, A. J.; Harvey, J. N. Non-Equilibrium Reaction and Relaxation Dynamics in a Strongly Interacting Explicit Solvent: F + CD_3DN Modelled with a Parallel Multi-State EVB Model. *J. Chem. Phys.* **2015**, *143*, 044120.

(7) Dunning, G. T.; Murdock, D.; Greetham, G. M.; Clark, I. P.; Orr-Ewing, A. J. Solvent Response to Fluorine-Atom Reaction Dynamics in Liquid Acetonitrile. *Phys. Chem. Chem. Phys.* **2015**, *17*, 9465−9470.

(8) Dunning, G. T.; Glowacki, D. R.; Preston, T. J.; Greaves, S. J.; Greetham, G. M.; Clark, I. P.; Towrie, M.; Harvey, J. N.; Orr-Ewing, A. J. Vibrational Relaxation and Microsolvation of DF after F-Atom Reactions in Polar Solvents. *Science* **2015**, *347*, 530−533.

(9) Morris, V. R.; Mohammad, F.; Valdry, L.; Jackson, W. M. Steric Effects on Nascent Vibrational Distributions of the HCN Product Produced in CN Radical Reactions with Ethane, Propane and Chloroform. *Chem. Phys. Lett.* **1994**, *220*, 448−454.

(10) Few, J. *FTIR Studies of Chemical Processes*. D.Phil. Thesis, University of Oxford: 2013.

(11) Copeland, L. R.; Mohammad, F.; Zahedi, M.; Volman, D. H.; Jackson, W. M. Rate Constants for CN Reactions with Hydrocarbons and the Product HCN Vibrational Populations: Examples of Heavy-Light-Heavy Abstraction Reactions. *J. Chem. Phys.* **1992**, *96*, 5817−5826.

(12) Bethardy, G. A.; Northrup, F. J.; Macdonald, R. G. The Initial Vibrational Level Distribution and Relaxation of $HCN[X^1\Sigma^+(v_10v_3)]$ in the $CN(X^2\Sigma^+)+CH_4 \rightarrow HCN+CH_3$ Reaction System. *J. Chem. Phys.* **1996**, *105*, 4533−4549.

(13) Bethardy, G. A.; Northrup, F. J.; Macdonald, R. G. The Initial Vibrational-State Distribution of HCN $X^1\Sigma^+(v_10v_3)$ from the Reaction $CN(X^2\Sigma^+)+C_2H_6 \rightarrow HCN+C_2H_5$. *J. Chem. Phys.* **1995**, *102*, 7966−7982.

(14) Bethardy, G. A.; Northrup, F. J.; He, G.; Tokue, I.; Macdonald, R. G. Initial Vibrational Level Distribution of $HCN[X^1\Sigma^+(v_10v_3)]$ from the $CN(X^2\Sigma^+)+H_2 \rightarrow HCN+H$ Reaction. *J. Chem. Phys.* **1998**, *109*, 4224−4236.

(15) Preston, T. J.; Hornung, B.; Pandit, S.; Harvey, J. N.; Orr-Ewing, A. J. Dynamical Effects and Product Distributions in Simulated CN + Methane Reactions. *J. Phys. Chem. A* 2015, submitted for publication.

(16) Glowacki, D. R.; Orr-Ewing, A. J.; Harvey, J. N. Product Energy Deposition of CN + Alkane H Abstraction Reactions in Gas and Solution Phases. *J. Chem. Phys.* **2011**, *134*, 214508.

(17) Rose, R. A.; Greaves, S. J.; Oliver, T. A. A.; Clark, I. P.; Greetham, G. M.; Parker, A. W.; Towrie, M.; Orr-Ewing, A. J. Vibrationally Quantum-State-Specific Dynamics of the Reactions of CN Radicals with Organic Molecules in Solution. *J. Chem. Phys.* **2011**, *134*, 244503.

(18) Rose, R. A.; Greaves, S. J.; Abou-Chahine, F.; Glowacki, D. R.; Oliver, T. A. A.; Ashfold, M. N. R.; Clark, I. P.; Greetham, G. M.; Towrie, M.; Orr-Ewing, A. J. Reaction Dynamics of CN Radicals with Tetrahydrofuran in Liquid Solutions. *Phys. Chem. Chem. Phys.* **2012**, *14*, 10424−10437.

(19) Greaves, S. J.; Rose, R. A.; Oliver, T. A. A.; Glowacki, D. R.; Ashfold, M. N. R.; Harvey, J. N.; Clark, I. P.; Greetham, G. M.; Parker, A. W.; Towrie, M.; Orr-Ewing, A. J. Vibrationally Quantum-State-Specific Reaction Dynamics of H Atom Abstraction by CN Radical in Solution. *Science* **2011**, *331*, 1423−1426.

(20) Dunning, G. T.; Preston, T. J.; Greaves, S. J.; Greetham, G. M.; Clark, I. P.; Orr-Ewing, A. J. Vibrational Excitation of Both Products of the Reaction of CN Radicals with Acetone in Solution. *J. Phys. Chem. A* **2015**, DOI: 10.1021/acs.jpca.5b05624.

(21) Coulter, P. C.; Grubb, M. P.; Koyama, D.; Orr-Ewing, A. J. Dynamics of Solvation, Reaction and Recombination of the Photoproducts of ICN in Solution. *J. Phys. Chem. A* **2015**, DOI: 10.1021/acs.jpca.5b10716.

(22) Raftery, D.; Gooding, E.; Romanovsky, A.; Hochstrasser, R. M. Vibrational Product State Dynamics in Solution-Phase Bimolecular Reactions - Transient Infrared Study of CN Radical Reactions. *J. Chem. Phys.* **1994**, *101*, 8572−8579.

(23) Crowther, A. C.; Carrier, S. L.; Preston, T. J.; Crim, F. F. Time-Resolved Studies of the Reactions of CN Radical Complexes with Alkanes, Alcohols, and Chloroalkanes. *J. Phys. Chem. A* **2009**, *113*, 3758−3764.

(24) Crowther, A. C.; Carrier, S. L.; Preston, T. J.; Crim, F. F. Time-Resolved Studies of CN Radical Reactions and the Role of Complexes in Solution. *J. Phys. Chem. A* **2008**, *112*, 12081−12089.

(25) Rosenthal, S. J.; Xie, X. L.; Du, M.; Fleming, G. R. Femtosecond Solvation Dynamics in Acetonitrile: Observation of the Inertial Contribution to the Solvent Response. *J. Chem. Phys.* **1991**, *95*, 4715−4718.

(26) Bagchi, B.; Jana, B. Solvation Dynamics in Dipolar Liquids. *Chem. Soc. Rev.* **2010**, *39*, 1936−1954.

(27) Greetham, G. M.; Burgos, P.; Cao, Q.; Clark, I. P.; Codd, P. S.; Farrow, R. C.; George, M. W.; Kogimtzis, M.; Matousek, P.; Parker, A. W.; et al. ULTRA: A Unique Instrument for Time-Resolved Spectroscopy. *Appl. Spectrosc.* **2010**, *64*, 1311−1319.

(28) Roberts, G. M.; Marroux, H. J. B.; Grubb, M. P.; Ashfold, M. N. R.; Orr-Ewing, A. J. On the Participation of Photoinduced N−H Bond Fission in Aqueous Adenine at 266 and 220 nm: A Combined Ultrafast Transient Electronic and Vibrational Absorption Spectroscopy Study. *J. Phys. Chem. A* **2014**, *118*, 11211−11225.

(29) Frisch, M. J.; Trucks, G. W.; Schlegel, H. B.; Scuseria, G. E.; Robb, M. A.; Cheeseman, J. R.; Scalmani, G.; Barone, V.; Mennucci, B.; Petersson, G. A.; et al. *Gaussian 09*; Gaussian Inc.: Wallingford, CT, 2009.

(30) Rivera, C. A.; Winter, N.; Harper, R. V.; Benjamin, I.; Bradforth, S. E. The Dynamical Role of Solvent on the ICN Photodissociation Reaction: Connecting Experimental Observables Directly with Molecular Dynamics Simulations. *Phys. Chem. Chem. Phys.* **2011**, *13*, 8269−8283.

(31) Grubb, M. P.; Orr-Ewing, A. J.; Ashfold, M. N. R. Koala: A New Program for the Processing and Decomposition of Transient Spectra. *Rev. Sci. Instrum.* **2014**, *85*, 064104.

(32) Moskun, A. C.; Bradforth, S. E. Photodissociation of ICN in Polar Solvents: Evidence for Long Lived Rotational Excitation in Room Temperature Liquids. *J. Chem. Phys.* **2003**, *119*, 4500−4515.

(33) Samuni, U.; Kahana, S.; Fraenkel, R.; Haas, Y.; Danovich, D.; Shaik, S. The ICN-INC System - Experiment and Quantum-Chemical Calculations. *Chem. Phys. Lett.* **1994**, *225*, 391−397.

(34) Larsen, J.; Madsen, D.; Poulsen, J.; Poulsen, T. D.; Keiding, S. R.; Thøgersen, J. The Photoisomerization of Aqueous ICN Studied by Subpicosecond Transient Absorption Spectroscopy. *J. Chem. Phys.* **2002**, *116*, 7997−8005.

(35) Helbing, J.; Chergui, M.; Fernandez-Alberti, S.; Echave, J.; Halberstadt, N.; Alberto Beswick, J. A. Caging and Excited State Emission of ICN Trapped in Cryogenic Matrices: Experiment and Theory. *Phys. Chem. Chem. Phys.* **2000**, *2*, 4131−4138.

(36) Helbing, J.; Chergui, M. Spectroscopy and Photoinduced Dynamics of ICN and Its Photoproducts in Solid Argon. *J. Phys. Chem. A* **2000**, *104*, 10293−10303.

(37) NIST Chemistry Webbook, NIST Standard Reference Database Number 69. http://webbook.nist.gov.

(38) Owrutsky, J. C.; Raftery, D.; Hochstrasser, R. M. Vibrational Relaxation Dynamics in Solutions. *Annu. Rev. Phys. Chem.* **1994**, *45*, 519−555.

(39) Andersson, M. P.; Uvdal, P. New Scale Factors for Harmonic Vibrational Frequencies Using the B3LYP Density Functional Method with the Triple-ζ Basis Set 6-311+G(d,p). *J. Phys. Chem. A* **2005**, *109*, 2937−2941.

(40) Trevitt, A. J.; Soorkia, S.; Savee, J. D.; Selby, T. S.; Osborn, D. L.; Taatjes, C. A.; Leone, S. R. Branching Fractions of the $CN+C_3H_6$ Reaction Using Synchrotron Photoionization Mass Spectrometry: Evidence for the 3-Cyanopropene Product. *J. Phys. Chem. A* **2011**, *115*, 13467−13473.

(41) Trevitt, A. J.; Goulay, F.; Meloni, G.; Osborn, D. L.; Taatjes, C. A.; Leone, S. R. Isomer-Specific Product Detection of CN Radical Reactions with Ethene and Propene by Tunable VUV Photoionization Mass Spectrometry. *Int. J. Mass Spectrom.* **2009**, *280*, 113−118.

(42) Gannon, K. L.; Glowacki, D. R.; Blitz, M. A.; Hughes, K. J.; Pilling, M. J.; Seakins, P. W. H Atom Yields from the Reactions of CN

Radicals with C_2H_2, C_2H_4, C_3H_6, Trans-2-C_4H_8, and *Iso*-C_4H_8. *J. Phys. Chem. A* **2007**, *111*, 6679−6692.

(43) Estillore, A. D.; Visger, L. M.; Kaiser, R. I.; Suits, A. G. Crossed-Beam Imaging of the H Abstraction Channel in the Reaction of CN with 1-Pentene. *J. Phys. Chem. Lett.* **2010**, *1*, 2417−2421.